Oral bioavailability enhancement of flubendazole by developing nanofibrous solid dosage forms

Article *in* Drug Development and Industrial Pharmacy · February 2017

DOI: 10.1080/03639045.2017.1298121

15 authors, including:

Tamás Vigh
Janssen Pharmaceutica
32 PUBLICATIONS **436** CITATIONS
SEE PROFILE

Balázs Démuth
Budapest University of Technology and Economics
30 PUBLICATIONS **302** CITATIONS
SEE PROFILE

Attila Balogh
Budapest University of Technology and Economics
40 PUBLICATIONS **679** CITATIONS
SEE PROFILE

Dorián L. Galata
Budapest University of Technology and Economics
5 PUBLICATIONS **12** CITATIONS
SEE PROFILE

DRUG DEVELOPMENT AND INDUSTRIAL PHARMACY, 2017
http://dx.doi.org/10.1080/03639045.2017.1298121

Taylor & Francis
Taylor & Francis Group

RESEARCH ARTICLE

Oral bioavailability enhancement of flubendazole by developing nanofibrous solid dosage forms

Tamás Vigh[a], Balázs Démuth[a], Attila Balogh[a], Dorián L. Galata[a], Ivo Van Assche[b], Claire Mackie[b], Monica Vialpando[b], Ben Van Hove[b], Petros Psathas[b], Enikő Borbás[a], Hajnalka Pataki[a], Peter Boeykens[b], György Marosi[a], Geert Verreck[b] and Zsombor K. Nagy[a]

[a]Department of Organic Chemistry and Technology, Budapest University of Technology and Economics, Budapest, Hungary; [b]Drug Product Development, Janssen R&D, Beerse, Belgium

ABSTRACT

The bioavailability of the anthelminthic flubendazole was remarkably enhanced in comparison with the pure crystalline drug by developing completely amorphous electrospun nanofibres with a matrix consisting of hydroxypropyl-β-cyclodextrin and polyvinylpyrrolidone. The thus produced formulations can potentially be active against macrofilariae parasites causing tropical diseases, for example, river blindness and elephantiasis, which affect altogether more than a hundred million people worldwide. The bioavailability enhancement was based on the considerably improved dissolution. The release of a dose of 40 mg could be achieved within 15 min. Accordingly, administration of the nanofibrous system ensured an increased plasma concentration profile in rats in contrast to the practically non-absorbable crystalline flubendazole. Furthermore, easy-to-grind fibers could be developed, which enabled compression of easily administrable immediate release tablets.

ARTICLE HISTORY
Received 12 August 2016
Revised 18 February 2017
Accepted 19 February 2017

KEYWORDS
Nanofiber; electrospinning; bioavailability; dissolution; downstream; amorphization; immediate release

Introduction

In various low-income regions of Africa and Asia, more than a hundred million people suffer from human filarial infections, for example, onchocerciasis (OC, river blindness) and lymphatic filariasis (LF). LF threatens 947 million people, and currently 120 million people are infected by it. Forty million of them are disfigured as a complication[1]. Mackenzie and Geary point out in their exhaustive review article that the currently used ivermectin primarily kills the young worms (microfilariae) that cause OC and LF[2], while the adult worms can survive and produce offspring for many years. Furthermore, it has been shown that treatment with a microfilaricide can result in serious reactions in the central nervous system (such as coma and death) in patients co-infected with OC and loiasis[3]. Thus, a macrofilaricide is needed to combat tissue-resident parasites efficiently and safely.

The most appealing benzimidazole drug with regard to combating filarial parasites is flubendazole[2], which has been shown to be active against the pathogens causing OC[4] and to have essentially 100% efficacy as a macrofilaricide[2] when given parenterally. Parenteral administration is a concern because the subcutaneous administration of flubendazole causes intolerable pain[5], while intramuscular injections induce inflammation[4]. In addition, there is a serious shortage of qualified healthcare workers in developing countries[6], who could safely administer injections. Improper sterilization practice and lacking supplies of injection equipment have been reported in various countries of Africa by the WHO[7]. Therefore, the safer and more convenient enteral route would clearly be preferred in the countries affected by OC and LF. Unfortunately, the biological action of enterally given crystalline flubendazole is localized to the gastrointestinal (GI) lumen. The poor oral bioavailability necessitates reformulation using modern pharmaceutical platforms in order to achieve systemic effects and enable the treatment of the mentioned infections. Up to now, *enabling* solid dosage forms of disclosed composition have only been reported by Vialpando et al, who constructed ordered mesoporous silica and spray-dried the API with cellulose derivatives[8]. A potential enabling excipient is hydroxypropyl-β-cyclodextrin (HPβCD) because when this solubilizing agent was given to rats orally through an intragastric tube, the plasma concentration of flubendazole could be remarkably increased[9].

A modern platform for bioavailability enhancement is the nanofibrous amorphous solid solutions. Electrospinning (ES) of fibers has got emerging attention in the field of pharmaceutical engineering owing to its high throughput and typically less heat stress in comparison with spray drying. It can enhance the physical stability of a small molecular drug[10], maintain the viability of encapsulated living organisms[11], and sustain[12] or accelerate[13,14] drug release. The dissolution enhancement can be ascribed to the high specific surface area generated[10,15–19]. Furthermore, the API likely solidifies as amorphous during the process, leading to a higher theoretical solubility and faster dissolution. The process of ES has been described in a couple of review articles[20–25]. It must also be noted that over decades, the ES process has had several serious limitations with regard to its application in the pharmaceutical industry. One of these was its extremely low productivity. Recently, there have been several attempts for the large-scale production of drug-loaded fibers, such as the free surface ES[26], pressurized gyration[27], and corona ES[28]. A milestone was reached toward the realization of pharma industry-compatible ES when the

CONTACT Geert Verreck gverreck@its.jnj.com Drug Product Development, Janssen R&D, Turnhoutseweg 30, 2340 Beerse, Belgium; Zsombor K. Nagy zsknagy@oct.bme.hu Department of Organic Chemistry and Technology, Budapest University of Technology and Economics, 1111 Budapest, Műegyetem rkp. 3–9, Hungary

high-speed electrospinning (HSES) process was developed[29]. It has been proven that HSES makes ES advantageously scalable, possibly up to a daily productivity of ~10 kg. With this throughput the technology can be part of continuous manufacturing lines assisted by process analytics, similar to the concept of GEA[30,31] and Glatt/ThermoHaake[32]. Another possible limitation of an ES process can be the grindability of the resulting nanofibrous solid dispersions. This property is essential when the solid dispersion is to be homogenized with excipients and dosed, that is, filled into capsules or compressed into tablets[33].

Flubendazole is currently used to kill worms that are present in the GI tract. Therefore, it acts locally, and requires no bioavailability. The aim of this work was to develop a solid, orally administrable dosage form of flubendazole that facilitates high oral bioavailability and hence may enable the systemic treatment of human filarial infections. Dissolution enhancement was to be ensured by embedding the drug into completely amorphous nanofibres of high specific surface area by ES. Then the products were to be tested for oral bioavailability. Tabletting experiments were to be carried out to check the feasibility of downstream processing and prepare final dosage forms. Ensuring grindability was a major point in facilitating the downstream processing. Dissolution from tablets was examined in order to reveal any significant changes in comparison with neat fibers.

Materials and methods

Materials

Crystalline flubendazole was supplied by Janssen Pharmaceutica Inc. (Beerse, Belgium). The compound has a molar weight of 313 g/mol, a melting point of 244 °C, a log *P* of 3[34] and pK_a values of 3.6 and 9.6[35]. Its solubility was found to be 29.6 mg/L in pH 1.2 HCl/KCl and 5.8 mg/L in pH 7.4 KH_2PO_4 buffer at 25 °C[36]. It is practically insoluble in common ES solvents such as ethanol and methanol, but well soluble in dimethyl formamide (5.6 g/L), dimethyl sulphoxide (15 g/L) and formic acid (340.5 g/L)[37].

Polyvinylpyrrolidone K90 (PVP) (Kollidon® 90 F) and Kollidon® CL were produced by BASF (Ludwigshafen, Germany). 2-Hydroxypropyl-β-cyclodextrin and mannitol were supplied by Roquette (Lestrem, France). Hydroxypropyl methylcellulose (HPMC 2910, Benecel™ E5) was purchased from Aqualon Hercules (Zwijndrecht, the Netherlands), and had a degree of methoxy substitution between 28.0% and 30.0%, and a degree of hydroxypropyl substitution between 7.0 and 12.0%. Microcrystalline cellulose (Vivapur® 200) purchased from JRS Pharma (Rosenberg, Germany). Aerosil® 200 was obtained from Evonik (Portland, OR) and Mg stearate from Sigma–Aldrich (Budapest, Hungary). The ES solvents were of reagent grade, the chromatographic eluents were of HPLC grade, and they were purchased from Merck Kft. (Budapest, Hungary).

Electrospinning of nanofibres

Flubendazole was embedded into nanofibrous solid forms using ES at two scales: single-needle electrospinning (SNES) and high-speed electrospinning (HSES). The common solution of flubendazole and the excipients was loaded into syringes and fed at a constant rate (0.8 ml/h for SNES and 200 ml/h for HSES) with a syringe pump (SEP-10 S Plus, Aitecs, Vilnius, Lithuania) onto a spinneret at ambient temperature. A high voltage supply (NT-35 High Voltage DC Supply, MA 2000, Unitronik Ltd., Nagykanizsa, Hungary) applied electric tension (40–50 kV) between the spinneret and an earthed aluminum sheet, which was used to collect the fine fibers. The collector was flat and rectangle-shaped (SNES: 300 × 250 mm, HSES: 600 × 400 mm). The collector-nozzle distance was 400 mm. After production, the electrospun fibers could be easily removed from the aluminum sheet and used for analytical examinations or downstream processing.

In the case of SNES, the spinneret was a single needle with an inner hole diameter of 0.5 mm. As for HSES (Quick2000 Ltd., Tiszavasvári, Hungary), the spinneret had sharp edges and a spherical cap geometry ($d = 55$ mm), connected to a high-speed motor. The rotational speed (25,000 rpm) of the spinneret was fixed during each experiment. Besides electrostatic effect, centrifugal force elongated the fibers, making this technology able to produce fibers at a higher flow rate. The electrospun fibers was milled with a pestle in a ceramic mortar.

The particle size distribution of the HSES fibers was examined on a Malvern Mastersizer 2000 (Malvern Instruments Ltd., Worcestershire, UK) particle size analyzer. About 1 g material was weighed and a basket equipped with metal balls was placed after the sample tray to facilitate the disaggregation of particles.

High performance liquid chromatography

0.1 g of crystalline starting flubendazole or fibrous products equivalent to this drug amount were dissolved in a 100.0 ml volumetric flask using dimethylformamide. 10 µl of the solution was injected onto the Agilent Eclipse Plus C18 column (3.5 µm; 100 mm × 4.6 mm) of an Agilent 1200 series HPLC system. The column was thermostated to 40 °C. The mobile phase A was a 7.5 g/L solution of ammonium acetate in water, and the mobile phase B was acetonitrile. Elution was performed as follows (time, mobile phase B): 0–15 min, 10–25%; 15–30 min, 25–55%; 30–32 min, 55–90%; 32–37 min, 90–90%, 37–38 min, 90–10%; >38 min, 10%. The flow rate was 1.2 ml/min. Chromatograms were recorded at 250 nm using an Agilent 1200 series Diode Array Detector (G1315B).

Scanning electron microscopy

Microscopic sample morphology was investigated by means of a JEOL 6380LVa (JEOL, Tokyo, Japan) type scanning electron microscope. Each specimen was fixed with conductive double-sided carbon adhesive tape and sputtered with gold or gold–palladium alloy (using a JEOL 1200 instrument) in order to avoid electrostatic charging.

X-ray powder diffraction

The flubendazole formulations were investigated with a PANalytical X'pert Pro MPD X-ray diffractometer (PANalytical, Almelo, the Netherlands) equipped with an X'Celerator detector with 0.04 sollers, using Cu Kα radiation (1.542 Å) and Ni filter. The applied voltage and current were 40 kV and 30 mA, respectively. The samples were analyzed between 4° and 42° 2θ in reflection mode. Automatic divergence and anti-scatter slits were used to provide 20 mm irradiated length.

In vitro *drug dissolution*

Pharmacopeia dissolution (fibers and tablets)

Dissolution of the starting crystalline flubendazole and drug release from the nanofibrous formulations or the tablets were

tested using a PTWS 600 instrument (Pharma Test Apparatebau AG, Hainburg, Germany). The nanofibres were ground in a mortar before the measurements. Each sample contained 40 mg of flubendazole. The dissolution medium was 900 ml of 0.1 M HCl maintained at a temperature of (37.0 ± 0.5) °C and stirred with a speed of 100 rpm. For crystalline flubendazole, the nanofibres and the tablets, the apparatus was a recently reported combination of the paddle and the basket apparatus, called "tapped basket"[29]. In accordance with common practice, a calibrated UV-Vis method was used to quantify the concentration of the drug, at a wavelength where no interference was found with excipient absorption. The absorption of the API in the dissolution medium was measured on-line at a wavelength of 282 nm with a Hewlett-Packard HP 8453 G UV-VIS spectrophotometer (Hewlett-Packard Enterprise, Palo Alto, CA,) after filtering (10 μm).

Small-volume dissolution of fibers

In order to model *in vitro* what maximum transient concentration can be reached in a small volume of dissolution medium (e.g. rat stomach), 5 mg of the starting crystalline flubendazole or ground nanofibrous formulation containing 50 mg of flubendazole was added to 20 ml of pH 2 HCl containing 0.5% HPMC, filled into a 50 ml vial. (The nanofibres were ground in a mortar before the measurement.) The closed vial was shaken manually for 30 s to facilitate dissolution. Then, the dissolution medium was maintained at ambient temperature without stirring. Samples were taken and filtered (1 μm) at given time points, then the concentration of the API in the dissolution medium was measured at-line at a wavelength of 282 nm with a Hewlett-Packard HP 8453 G UV-VIS spectrophotometer (Hewlett-Packard Enterprise, Palo Alto, CA).

Pharmacokinetics in rats

All animal studies were completed under appropriate national and international guidelines. The Local Ethical Committee in compliance with the Declaration of Helsinki approved all in vivo studies. Male Sprague-Dawley ($n = 3$) rats were dosed (20 mg/kg) by gavage with each formulation of interest suspended in 0.5% HPMC to improve wetting. The vehicle contained 2 mg/ml drug. At various time points (30 min, 1, 2, 4, 7 and 24 h) blood was collected from the tail vein into Microvette tubes. Sample were centrifuged to separate plasma, and placed subsequently (within 1 h) in the freezer until analyzed. The bioanalytical method consisted of protein precipitation and subsequent LC-MS/MS analysis: to 10.0 μl aliquots of plasma, 50 μl of DMSO standard solution was added for calibration, and 50 μl of DMSO was added to all other samples. 25 μl of stable isotope labeled flubendazole (100 ng/ml) in methanol was added to all samples as an internal standard, except to single blanks without IS, which received 25 μl of methanol. Precipitation of the plasma proteins was carried out by addition of 400 μl of acetonitrile after which the samples were vortex-mixed and centrifuged. 5 μl of the supernatant was injected onto a 50 mm × 2.1 mm X-BridgeC18 column with 3.5 μm particles. The mobile phase consisted of 0.1% formic acid (mobile phase constituent A) and acetonitrile (mobile phase constituent B). A 2.5-min gradient from 25% B to 50% B was followed by a 1-min step gradient to 98% B and a 1.5-min re-equilibration to the initial conditions. The flow rate was 0.4 ml/min. MS/MS analysis was performed using a Sciex API4000 triple quadrupole mass spectrometer in the Multiple Reaction Monitoring (MRM) mode, optimized for the compounds. The mass transitions for API and the stable isotope labeled internal standard were m/z 314.1–282.0 and 317.1–282.0, respectively. Samples were quantified against calibration curves and quality control samples prepared to cover the concentration range of the study samples. The curves and quality control samples were prepared in the same matrix as the study samples. The lower limit of quantitation was 5.00 ng/ml for the API, and the calibration range was 5.00–5000 ng/ml.

Data on drug levels obtained from plasma samples were normalized for the amount of compound administered, the weight of the individual animals and used to determine a number of pharmacokinetic parameters using WinNonlin® Professional (Pharsight, Mountain View, CA). A non-compartmental analysis using the log-linear trapezoid rule with a log-linear extrapolation was applied.

Tablet compression and characterization

The fibrous solid dispersion of flubendazole was ground and homogenized with tableting excipients. The tablets were compressed with a CTR-6 press (Dott. Bonapace, Limbiate, Italy) equipped with 14 mm concave punches. The compression force was monitored and recorded real-time.

The Carr index of the tableting mixture was measured using a 250 ml graduated cylinder. One hundred milliliters of the material were weighed, and the volume of tapped powder was measured after 1250 taps on an ERWEKA SVM12 tapping volumeter (Erweka, Heusenstamm, Germany). The hardness of tablets was measured with a Schleuniger 4 M hardness tester using the average of $n = 5$. Friability was examined on a PharmaTest PTF E friability test apparatus with 10 tablets after 300 rounds. Outflow time was measured with a powder amount of 100 g on a gently shaken metal funnel with a 10 mm orifice using the average of $n = 3$.

Results and discussion

Electrospinning and characterization of flubendazole solid dispersions

Electrospun amorphous nanofibres of flubendazole were developed in order to accelerate the dissolution of the drug. Therefore, the matrix components were selected from among hydrophilic materials. PVP was a promising candidate owing to its outstanding spinnability[16]. In an earlier study[17], the well wettable 2-hydroxypropyl-β-cyclodextrin (HPβCD) could be used advantageously beside PVP to accelerate drug release and prevent drug crystallisation during dissolution. Furthermore, the complexing agent has been shown to increase the apparent solubility of flubendazole[36] and its bioavailability when administered as oral solution[9].

As the API does not dissolve in ethanol, with which the ES of HPβCD/PVP systems has been described[17], a new method had to be developed using the best solvent of the drug. It is formic acid (HCOOH), which belongs to the same toxicity class of residual solvents as ethanol[38]. HCOOH dissolves the API and the excipients very well, and even an HPβCD/PVP ratio as high as 4:1 could be ensured. Replacing a small fraction of HCOOH with ethanol was found to be advantageous with regard to processability. Fibres with drug loads of 10 and 20% could be produced using the single-needle setup, SNES (Table 1). The HPβCD/API mass ratio was 7.2 and 3.2, respectively.

The process could be scaled up from a feed rate of 0.8 ml/h to 200 ml/h by changing the ES setup from the single-needle ES to the high-speed ES instrument[29]. This means an increase in productivity from 0.8 ml/h to 200 ml/h. The scale-up did not affect fiber morphology notably, as shown in Figure 1. Both SNES and HSES delivered fibers of diameters less than 500 nm. While this size is

Table 1. Electrospinning of HPβCD/PVP K90 fibers with flubendazole.

Formulation	API (%)	HPβCD (%)	PVP K90 (%)	EtOH (ml/g)	HCOOH (ml/g)	Throughput (ml/h)	Voltage (kV)	Setup
SNES_10%	10	72	18	0.18	3.6	0.8	40	SNES
SNES_20%	20	64	16	0.16	3.2	0.8	40	SNES
HSES_10%	10	72	18	0.18	3.6	200	50	HSES
HSES_20%	20	64	16	0.16	3.2	200	50	HSES

SNES: single-needle electrospinning; HSES: high-speed electrospinning; temperature: 25 °C.

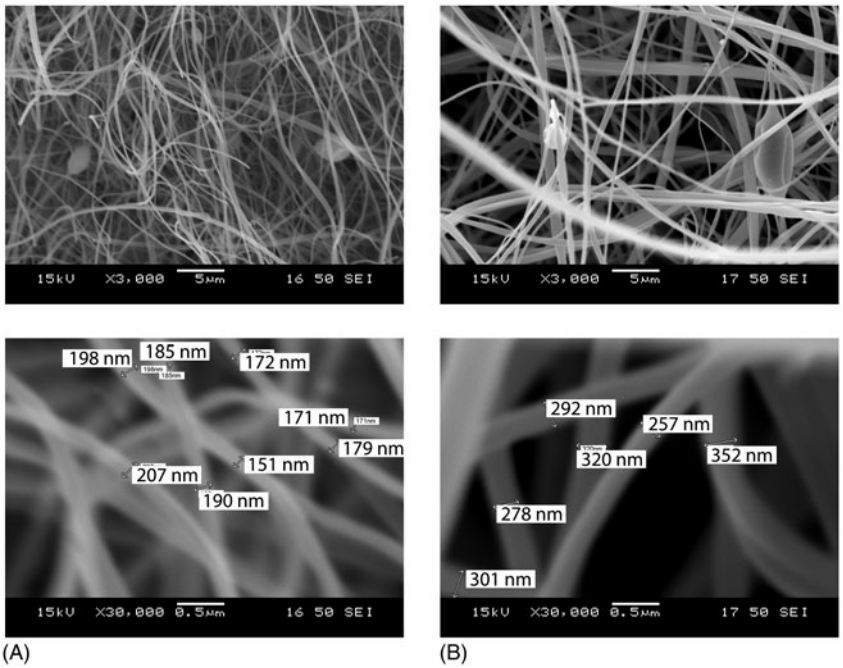

Figure 1. Scanning electron micrographs of (A) SNES_20% and (B) HSES_20%.

still small enough to generate a high specific surface area for dissolution enhancement, the fibers were not extremely thin, which can be beneficial with respect to grindability.

Macroscopically, the fibers are prone to agglomerate and form larger particles. The particle size analysis showed 8.42, 113.94 and 626.38 μm for d(0.1), d(0.5) and d(0.9) values, respectively. These values thus belong to spontaneously formed loose agglomerates not the individual fibers.

The fibers were electrospun from a multi-component acidic solution, where chemical reactions take place more likely than in the solid state. Therefore, it was necessary to check, before proceeding with examinations, whether flubendazole underwent notable chemical degradation during processing. Therefore, chromatographic investigations were performed based on a Ph. Eur. method.

Figure 2 shows that the chromatograms of the formulations were very similar to that of crystalline flubendazole. While the summed integral of impurities was (330 ± 2) mAUs in the case of the starting material, (341 ± 18) mAUs and (316 ± 4) mAUs were measured in the case of SNES_10% and SNES_20%. Thus, the conclusion can be drawn that no considerable decomposition occurred during ES. Therefore, the decision was taken to carry out further characterization on the products, including measuring *in vitro* and in vivo profiles. The results also indicate that the applied ES process will be feasible to produce samples for a future toxicological investigation.

Powder X-ray diffraction examinations were carried out to prove that flubendazole underwent complete amorphisation during the ES process. The curves in Figure 3 show that no crystalline API was present in the fibers in an observable amount, and devitrification occurred neither in 1 month, nor in 3 and 5 months. The demonstrated physical stability is necessary to prevent the aimed immediate dissolution from spoiling.

Examination of in vitro *drug release and* in vivo *bioavailability*

It is a huge technological advantage over most electrospun systems that the flubendazole nanofibres were developed to be grindable in this study. This way the amorphous solid solutions can be easily fed into and handled in downstream processing units, such as a blender and a tablet press. Before the ground solid dispersions were further processed, their dissolution and bioavailability were studied.

In comparison with the very slow *in vitro* dissolution of crystalline flubendazole, the drug release was rapid from the ground HSES_10% and HSES_20% formulations in acidic medium. Figure 4 shows that 80% of the 40 mg flubendazole load dissolved in 3 min, and total release could be achieved in 15 min, while no precipitation occurred afterwards. In contrast, only 12.16 mg of the crystalline drug could be dissolved in 120 min under the same circumstances.

The excellent *in vitro* dissolution results of the nanofibrous formulations encouraged us to test the solid dispersions *in vivo* in rats. However, before performing the animal studies, a further *in vitro* investigation was done to find out the maximum transient concentration that can be reached in a small volume of dissolution medium. Knowing that the gastric volume of 500 g adult Sprague–Dawley male rats is about 18 ml[39], the ground

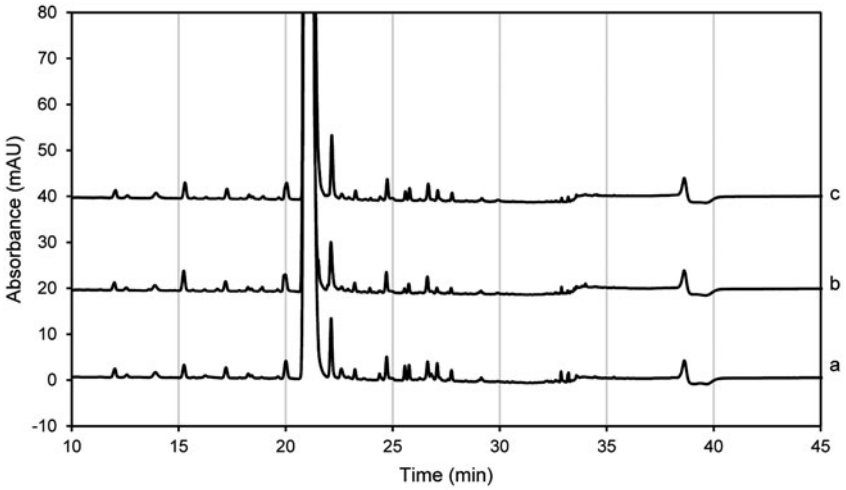

Figure 2. HPLC chromatograms of (a) starting crystalline flubendazole, (b) SNES_10%, (c) SNES_20%.

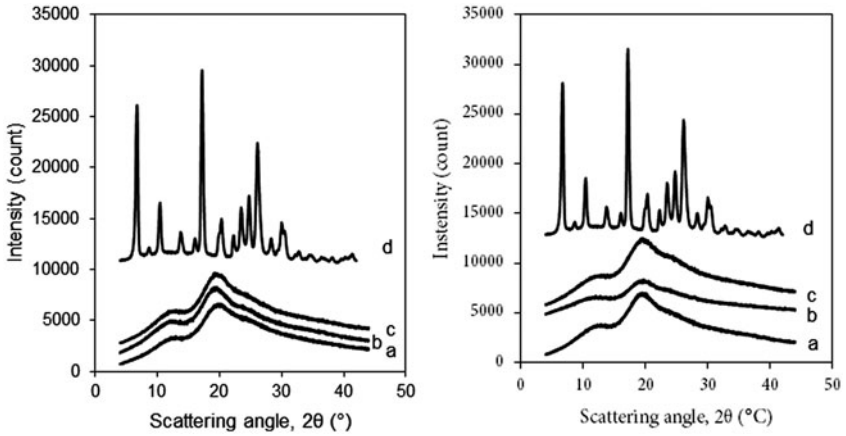

Figure 3. PXRD scattering curves of (A) HSES_10% and (B) HSES_20% after a storage of (a) 1 month, (b) 3 months and (c) 5 months. The diffractogram of crystalline flubendazole is displayed as a reference (d).

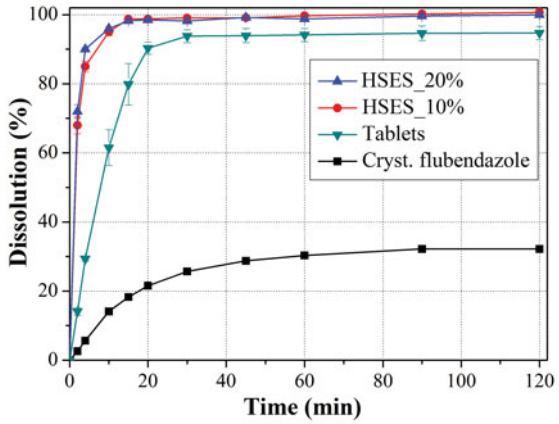

Figure 4. Dissolution curves belonging to crystalline starting flubendazole, the ground fibrous formulations containing 10% and 20% API and the tableted solid dispersions at pH 1.0 and a dose of 40 mg.

formulations with a dose of 50 mg were dissolved in only 20 ml of a pH 2 medium (the minimum pH of gastric juice in rats[40,41]). No total dissolution could be reached with HSES_20% in which the HPβCD:API mass ratio was 3.2 (1st photo, bottom line, Figure 5), and even the dissolved part started precipitating at about 90 min (2nd photo, bottom line, Figure 5). In turn, when HSES_10% with a HPβCD:API mass ratio of 7.2 was brought into contact with the medium, an almost transparent solution could be obtained in a time as short as 30 min (upper line, Figure 5). An extremely high concentration (2000 mg/L) far exceeding the equilibrium solubility of pure crystalline flubendazole could be reached, without observable precipitation in 120 min. This is a huge advantage in comparison with the crystalline API, which did practically not dissolve. Therefore, the *in vivo* experiments were carried out using HSES_10%.

Ground HSES_10% was assessed in a rat model for its biopharmaceutical properties (Figure 6). Comparison was made against a flubendazole microsuspension described by Vialpando et al.[8] The results were in agreement with the *in vitro* studies. The fibrous system turned out to show a significantly higher blood level profile than the microcrystalline API. The HSES_10% powder generated an $AUC_{0-7\,h}$ of 7095 ng h/ml (CV 25%), a C_{max} of 2090 ng/ml (CV 15%) and a t_{max} of 0.75 h (CV 47%). With the microsuspension, AUC was (575 ± 60.5) ng h/ml, C_{max} was (102 ± 14.1) ng/ml and t_{max} was (3.0 ± 1.73) h.

The AUC and C_{max} belonging to the fibrous solid dispersion are more than one order of magnitude higher than that of the microcrystalline API. The remarkably increased bioavailability means that flubendazole has the potential to act systemically, for example against the parasites causing LF and OC, when formulated into solid electrospun fibers.

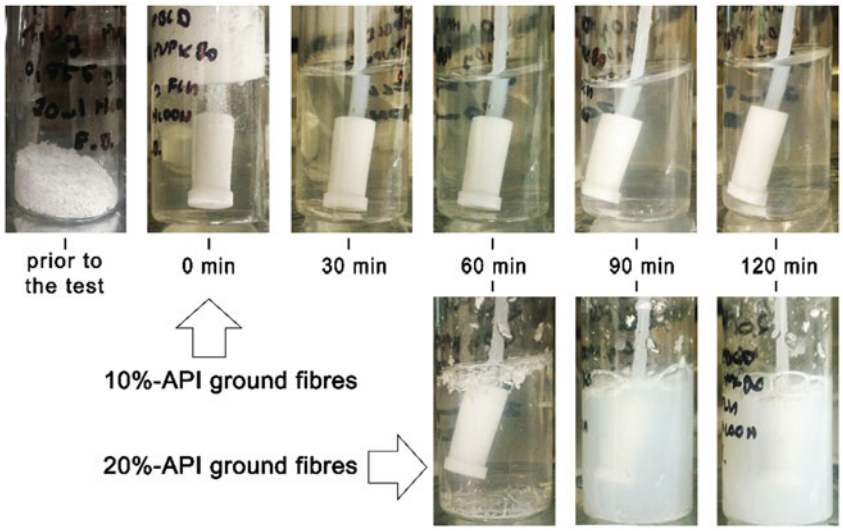

Figure 5. Dissolution of the 10%- and 20% flubendazole-containing ground nanofibres in an extra small volume of pH 2 dissolution medium. Upper line (10%-API fibers): clear solution 0, 30, 60, 90 and 120 min after the addition of solvent. Bottom line: (20%-API fibers): undissolved particles at 60 min, precipitated drug at 90 and 120 min.

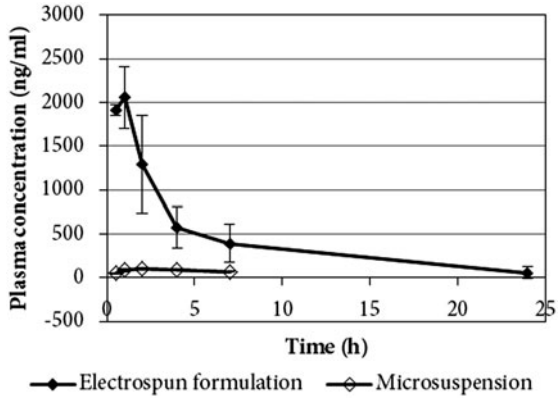

Figure 6. Plasma levels of flubendazole after a 20 mg/kg dose was administered as a nanospun dispersion (HSES_10%) by gavage in 0.5% HPMC with the vehicle containing drug in 2 mg/ml. Comparison is made with the microsuspension described by Vialpando et al.[8].

Table 2. Composition and characteristic attributes of the tableted mixtures and the compressed tablets.

Composition	Carr index	Outflow time (s/100 g)	Compression force (kg)	Tablet mass (mg)	Tablet hardness (N)	Friability (%)
HSES_10%: 40.00% Mannitol: 23.75% MCC: 23.75% Kollidon CL: 10.00% Aerosil 200: 1.00% Mg stearate: 1.50%	18.5	98 ± 5	~1200	500 (2×)	166 ± 9	0.44

Downstream processing of the flubendazole nanofibres

When the flubendazole nanofibres of enhanced bioavailability developed in this study are administered to humans as a systemic medication to combat filarial infections, easy-to-swallow solid dosage forms, such as tablets, will be preferred. The grindable nature of HSES_10% enabled its efficient homogenization with the mixture of tableting excipients of preliminarily optimized composition. Based on the Carr index and the time of funnel outflow, the mixture seemed to be suitable for tableting (Table 2).

For the determination of dose, literature data were taken into account. The effective dose (LED_{90}) of subcutaneously administered flubendazole against *Brugia malayi* was found to be 75 mg/m^2 in rats (given for 5 consecutive days)[42]. This worm is among the species causing LF[1]. By a rough estimation based on body surface area, an equivalent human dose of 2 mg/kg can be calculated with, that is, 120 mg daily for a 60 kg person. This suggests approx. 40 mg three times a day.

Tablets containing HSES_10% in an amount of 40% were compressed to the appropriate hardness of 166 ± 9 N (Table 2) and friability (0.44%). Automatic feeding was also feasible, the so obtained tablets had a weight variation of 11.8 mg. Kollidon CL was used as disintegrant, mannitol and microcrystalline cellulose (MCC) as filler, Aerosil 200 as glidant and Mg stearate as lubricant.

After tableting, the effect of this process on dissolution was investigated. Disintegration was complete in 6.75 min, and less than 8 min were enough to reach 80% dissolution (Figure 4). The release could be nearly completed in 20 min, which shows that the benefits of the tablet dosage form can be exploited while practically maintaining the enhanced dissolution profile that was found to be characteristic of the nanofibres.

Conclusions

The ultimate purpose of this on-going development is to design a high-productivity process for the production of a human anthelmintic dosage form, which can effectively treat tropical filarial infections, such as LF (elephantiasis) and OC (river blindness).

ES proved to be the first feasible approach to produce bioavailable solid formulations of the anthelminthic flubendazole. These potentiate the systemic treatment of widespread human filarial infections. The amorphous nanofibres based on HPβCD and PVP enabled 15-min drug release *in vitro* and resulted in significantly increased plasma concentration in rats in contrast to the practically non-absorbable crystalline flubendazole.

The remarkably enhanced bioavailability makes the electrospun nanoformulations a candidate worthy of toxicological studies. In case of a positive outcome, the easy-to-grind nature fibers can allow industrial scale milling and converting into tablets for trials without spoiling the ultrafast release, as shown by the tableting

experiment. However, large-scale manufacturing based on ES will necessitate a further scale-up beyond the 250-fold increase in throughput achieved in this study.

Acknowledgements

A strong foundation of this work was the stimulating professional enthusiasm of Dr. Marcus E. Brewster, former Vice President and Scientific Fellow at Janssen Research and Development.

The authors are indebted to Éva Kiserdei for her outstanding technical support. This work is connected to the scientific program of the "Development of quality-oriented and harmonized R + D+ I strategy and functional model at BME" project. The authors mean to express their gratitude to Dr János Madarász (Budapest University of Technology and Economics, Hungary) for making XRD measurements possible in his laboratory.

Disclosure statement

The authors report no conflicts of interest.

Funding

This project is supported by the New Széchenyi Plan (Project ID: TÁMOP-4.2.1/B-09/1/KMR-2010–0002), by OTKA research fund [grant number K112644], and by the János Bolyai Research Scholarship of the Hungarian Academy of Sciences.

References

1. World Health Organization. Fact sheet N°102 – lymphatic filariasis. Available from: http://www.who.int/mediacentre/factsheets/fs102/en/ [last accessed 6 Nov 2016].
2. Mackenzie CD, Geary TG. Flubendazole: a candidate macrofilaricide for lymphatic filariasis and onchocerciasis field programs. Expert Rev Anti Infect Ther 2011;9:497–501.
3. Mackenzie CD, Geary TG, Gerlach JA. Possible pathogenic pathways in the adverse clinical events seen following ivermectin administration to onchocerciasis patients. Filaria J 2003;2:S5.
4. Dominguez-Vazquez A, Taylor HR, Greene BM, et al. Comparison of flubendazole and diethylcarbamazine in treatment of onchocerciasis. Lancet 1983;1:139–43.
5. Goodwin LG. Chemotherapy. Trans R Soc Trop Med Hyg 1984;78:1–8.
6. Naicker S, Plange-Rhule J, Tutt RC, Eastwood JB. Shortage of healthcare workers in developing countries – Africa. Ethn Dis 2009;19:S1-60–64.
7. Dicko M, Oni A-QO, Ganivet S, et al. Safety of immunization injections in Africa: not simply a problem of logistics. Bull World Health Organ 2000;78:163–9.
8. Vialpando M, Smulders S, Bone S, et al. Evaluation of three amorphous drug delivery technologies to improve the oral absorption of flubendazole. J Pharm Sci 2016;105:2782–93.
9. Ceballos L, Elissondo M, Bruni SS, Denegri G, Alvarez L, Lanusse C. Flubendazole in cystic echinococcosis therapy: pharmaco-parasitological evaluation in mice. Parasitol Int 2009;58:354–8.
10. Balogh A, Horváthová T, Fülöp Z, et al. Electroblowing and electrospinning of fibrous diclofenac sodium-cyclodextrin complex-based reconstitution injection. J Drug Deliv Sci Technol 2015;26:28–34.
11. Nagy ZK, Wagner I, Suhajda Á, et al. Nanofibrous solid dosage form of living bacteria prepared by electrospinning. eXPRESS Polym Lett 2014;8:352–61.
12. Sóti PL, Nagy Z, Serneels K, et al. Preparation and comparison of spray dried and electrospun bioresorbable drug delivery systems. Eur Polym J 2015;68:671–9.
13. Nagy Z, Nyúl K, Wagner K, et al. Electrospun water soluble polymer mat for ultrafast release of Donepezil HCl. Express Polym Lett 2010;4:763–72.
14. Nagy ZK, Balogh A, Vajna B, et al. Comparison of electrospun and extruded soluplus®-based solid dosage forms of improved dissolution. J Pharm Sci 2012;101:322–32.
15. Yu DG, Zhu L, White M, Branford-White KC. Electrospun nanofiber-based drug delivery systems. Health 2009;1:67–75.
16. Yu D-G, Zhang X-F, Shen X-X, et al. Ultrafine ibuprofen-loaded polyvinylpyrrolidone fiber mats using electrospinning. Polym Int 2009;58:1010–13.
17. Vigh T, Horváthová T, Balogh A, et al. Polymer-free and polyvinylpirrolidone-based electrospun solid dosage forms for drug dissolution enhancement. Eur J Pharm Sci 2013;49:595–602.
18. Balogh A, Drávavölgyi G, Faragó K, et al. Plasticized drug-loaded melt electrospun polymer mats: characterization, thermal degradation, and release kinetics. J Pharm Sci 2014;103:1278–87.
19. Balogh A, Farkas B, Faragó K, et al. Melt-blown and electrospun drug-loaded polymer fiber mats for dissolution enhancement: a comparative study. J Pharm Sci 2015;104:1767–76.
20. Panthi G, Park M, Kim H-Y, Park S-J. Electrospun polymeric nanofibers encapsulated with nanostructured materials and their applications: a review. J Ind Eng Chem 2015;24:1–13.
21. Ghorani B, Tucker N. Fundamentals of electrospinning as a novel delivery vehicle for bioactive compounds in food nanotechnology. Food Hydrocoll 2015;51:227–40.
22. Sell SA, McClure M, Garg JK, et al. Electrospinning of collagen/biopolymers for regenerative medicine and cardiovascular tissue engineering. Adv Drug Deliv Rev 2009;61:1007–19.
23. Reneker DH, Yarin A, Zussman L, Xu EH. Electrospinning of nanofibers from polymer solutions and melts. Adv Appl Mech 2007;41:43–346.
24. Agarwal S, Greiner A, Wendorff JH. Functional materials by electrospinning of polymers. Prog Polym Sci 2013;38:963–91.
25. Reneker DH, Yarin AL. Electrospinning jets and polymer nanofibers. Polymer 2008;49:2387–425.
26. Brettmann B, Cheng KK, Myerson AS, Trout BL. Electrospun formulations containing crystalline active pharmaceutical ingredients. Pharm Res 2013;30:238–46.
27. Raimi-Abraham B, Mahalingam TS, Davies P, et al. Development and characterization of amorphous nanofiber drug dispersions prepared using pressurized gyration. Mol Pharm 2015;12:3851–61.
28. Molnar K, Nagy ZK. Corona-electrospinning: needleless method for high-throughput continuous nanofiber production. Eur Polym J 2016;74:279–86.
29. Nagy ZK, Balogh A, Démuth B, et al. High speed electrospinning for scaled-up production of amorphous solid dispersion of itraconazole. Int J Pharm 2015;480:137–42.
30. Vanhoorne V, Bekaert B, Peeters E, et al. Improved tabletability after a polymorphic transition of

delta-mannitol during twin screw granulation. Int J Pharm 2016;506:13–24.
31. Peeters E, Tavares da Silva A, Toiviainen F, et al. Assessment and prediction of tablet properties using transmission and backscattering Raman spectroscopy and transmission NIR spectroscopy. Asian J Pharm Sci 2016;11:547–58.
32. Leister D. Continuous granulation - opportunities to increase efficiency in pharmaceutical production. Pharma Bio World July 2011;42–46.
33. Démuth B, Nagy Z, Balogh K, et al. Downstream processing of polymer-based amorphous solid dispersions to generate tablet formulations. Int J Pharm 2015;486:268–86.
34. Grabowski T, Jaroszewski J, Piotrowski JW. Correlations between no observed effect level and selected parameters of the chemical structure for veterinary drugs. Toxicol Vitr 2010;24:953–9.
35. Lampo A, Vanparys P, van Cauteren H. Report on the safety documentation of flubendazole. A report written at Janssen Research Foundation, Beerse, 1996.
36. Ceballos L, Moreno L, Torrado JJ, et al. Exploring flubendazole formulations for use in sheep. Pharmacokinetic evaluation of a cyclodextrin-based solution. BMC Vet Res 2012;8:71–80.
37. Nobilis M, Jira T, Lísa M, et al. Achiral and chiral high-performance liquid chromatographic determination of flubendazole and its metabolites in biomatrices using UV photodiode-array and mass spectrometric detection. J Chromatogr A 2007;1149:112–20.
38. International Conference on Harmonisation of Technical Requirements for Registration of Pharmaceuticals for Human Use, Tripartite Guideline – Impurities: Guideline for Residual Solvents, Q3C(R5). Available from: http://www.ich.org/fileadmin/Public_Web_Site/ICH_Products/Guidelines/Quality/Q3C/Step4/Q3C_R5_Step4.pdf [last accessed 15 Mar 2015].
39. Bull LS, Pitts GC. Gastric capacity and energy absorption in the force-fed rat. J Nutr 1971;101:593–6.
40. Altman PL, Dittmer DS. Blood and other body fluids. In: Biological handbooks. Washington, DC: Federation of American Societies for Experimental Biology; 1961. p. 186.
41. Nebendahl K. Routes of administration. The laboratory rat. Elsevier; 2000:463–483.
42. Zahner H, Schares G. Experimental chemotherapy of filariasis: comparative evaluation of the efficacy of filaricidal compounds in *Mastomys coucha* infected with *Litomosoides carinii*, *Acanthocheilonema viteae*, *Brugia malayi* and *B. pahangi*. Acta Trop 1993;52:221–66.